Corner reflectors and Quantum-Non-Demolition Measurements in gravitational wave antennae

V. B. Braginsky and S. P. Vyatchanin
Physics Faculty, Moscow State University, Moscow 119992, Russia
e-mail: vyat@hbar.phys.msu.ru
(Dated: February 24, 2004)

We propose Fabry-Perot cavity with corner reflectors instead of spherical mirrors to reduce the contribution of thermoelastic noise in the coating which is relatively large for spherical mirrors and which prevents the sensitivity better than Standard Quantum Limit (SQL) from being achieved in laser gravitational wave antenna. We demonstrate that thermo-refractive noise in corner reflector (CR) is substantially smaller than SQL. We show that the distortion of main mode of cavity with CR caused by tilt and displacement of one reflector is smaller than for cavity with spherical mirrors. We also consider the distortion caused by small nonperpendicularity of corner facets and by optical inhomogeneity of fused silica which is proposed as a material for corner reflectors.

I. INTRODUCTION

The existing to-day's multi-layer dielectric coating on optical mirrors allows to realize very high resolution experiments (see e.g. [1]). The reflectivity R in the best optical coating has reached the level of $(1-R) \simeq 10^{-6}$ [1–3] (commercially available $(1-R) \simeq 10^{-5}$), and there are many reasons to expect that further improvement of coating technologies will permit to obtain the value of $(1-R) \simeq 10^{-9}$. With the value of $(1-R) \simeq 10^{-5}$ it is possible to realize the ring down time $\tau^*_{FP} \simeq 1$ sec in 4 km long Fabry-Perot (FP) resonators which are the basic elements in laser interferometer gravitational wave antennae (project LIGO [4, 5]). This relatively large value of τ^*_{FP} permits to have relatively small value of the ratio of $\sqrt{\tau_{av}/\tau^*_{FP}} \simeq 7\times 10^{-2}$ (if the averaging time $\tau_{av} \simeq 5\times 10^{-3}$ sec). This ratio is the limit for the squeezing factor which may be obtained if QND procedure of measurement in such FP resonator is used [6, 7]. Such a procedure will allow to circumvent the Standard Quantum Limit (SQL) of sensitivity (see details in [8]).

Few years ago the role of the thermoelastic noise in the bulk of the mirrors was analyzed [9]. This analysis has shown that if the laser beam spot size on the mirror surface is sufficiently large then the small value of the thermal expansion coefficient $\alpha_{SiO_2} \simeq 5\times 10^{-7}$ K^{-1} of fused silica will permit to circumvent the SQL sensitivity by the factor of $\simeq 0.1$ (if the thermoelastic noise is the only source of noises). The consequent analysis of thermoelastic noise in the coating itself unfortunately predicts that the limit of sensitivity will be close to the SQL of sensitivity [10–13]. The origin of this obstacle is relatively big numerical value of thermal expansion coefficient $\alpha_{Ta_2O_5} \simeq 5\times 10^{-6}$ K^{-1} of amorphous Ta_2O_5 [13] which is used in the best coatings as well as relatively big number of layers (usually 20-40) which is necessary to have small value of $(1-R)$. For LIGO project these limitations may be illustrated by the following numerical values. The SQL sensitivity of detectable amplitude of the perturbation of the metric is equal to [14]

$$\sqrt{S_h^{SQL}(\omega)} = \sqrt{\frac{8\hbar}{m\omega^2 L^2}} \simeq 2\times 10^{-24}\ \mathrm{Hz}^{-1/2}, \qquad (1.1)$$

where m = 40 kg is mass of test mass, L = 4 km is distance between them, $\omega = 2\pi\times 400\ \mathrm{s}^{-1}$ is observation frequency. Here and below the estimates are calculated for numerical parameters listed in Appendix F. At the same time, according to the measurement [13], the limit of sensitivity of such an antenna only due to the thermoelastic noise in the multi-layer $Ta_2O_5 + SiO_2$ coating on SiO_2 substrate has to be between [10]

$$\sqrt{S_h^{TD\,coat}(\omega)} \simeq (0.6 \div 1.4)\times 10^{-24}\ \mathrm{Hz}^{-1/2} \qquad (1.2)$$

The goal of this article is to present the analysis of another version of optical FP cavity where the "contribution" of the thermoelastic noise in coating is substantially reduced. The key idea of this version is based on concept of corner optical reflector (tri-hedral or two-hedral prism). These types of reflectors were well known among the jewelers at least from 16-th century (see e.g. autobiography by Benvenutto Cellini [15]). In the 70-s of the previous century corner reflectors (CR) installed on the Moon allowed to test the principle of equivalence for the gravitational defect of mass by laser ranging [16]. Here we propose to substitute mirrors with finite value of surface curvature (see fig.1 a) by 3 facets (fig.1 b) or 2 facets (see fig.1 c) corner reflectors (CR) manufactured from fused silica. For the same radius R_b of laser beam the mass of CR is about the same value as cylindrical mirrors (with height about equal to radius of cylinder) especially if idle parts of CR is removed. For example for 2 facets CR the size of foot surface has to be about 45×45 cm^2 with total test mass about 40 kg (the same as planned in advanced LIGO).

In the proposed scheme the stability of optical mode is provided by surfaces lens shaping of each CR foot (as shown in fig.2a). For reflectors manufactured from fused silica the total internal reflection inside the reflectors is possible because refraction index $n_{SiO_2} = 1.45$ is large enough (due to Snellius law): $n_{SiO_2}\sqrt{2/3} > 1$ for 3 facets reflector or $n_{SiO_2}\sqrt{1/2} > 1$ for 2 facets reflector.

In section II we consider the modes of ideal cavity (fig.2) and the distortion of the main mode structure caused by small perturbations of different kinds: tilt angle θ (fig. 3), displacement δx of one reflector (fig. 4), expose angle ϵ (fig.5).

In section III we compare these perturbations for cavities with spherical mirrors and with corner reflectors and give numerical estimates for the particular case of laser beam radius $R_b \simeq 6$ cm (intensity of beam decreases as e^{-1} at distance R_b from center) which is planned for Advanced

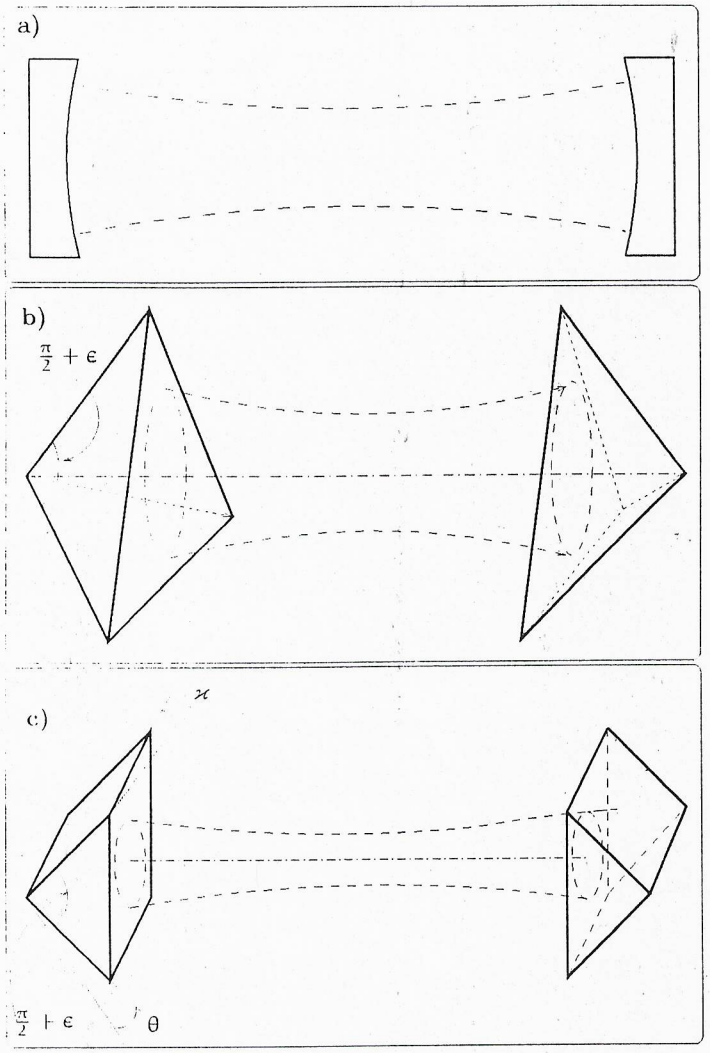

FIG. 1: We propose to replace mirrors with finite value of surface curvature (a) by 3 facets "triprism" type CR (b) or 2 facets "roof" type CR (c).

LIGO. Distortions of mode are undesirable in high accuracy spectroscopic measurements because they may produce additional noise. For example, in laser gravitational wave antenna the light beams from two independently perturbed FP cavities (placed in each arm of Michelson interferometer) will not produce completely zero field at the dark port after the beam splitter. It is equivalent to additional noise at the dark port.

In section IV we consider the different sources of optical losses of CR and show that they can be at level $(1-R)\simeq 10^{-5}$.

In cavity with CRs it is necessary to use nevertheless relatively thin anti-reflective coatings (2 – 4 layers) on lense shape foot. It has to be done to keep the value $(1-R)$ at the level $\simeq 10^{-5}$. Because this coating is substabtialy thiner than typical high reflective one (20 – 40 layers) used in curved mirrors, thermoelastic noise may be depressed by the factor ~ 10 i.e. about one order less than SQL (the estimate (1.2) is given for 38 layers). The "fee" for use of CR is the additional thermo-refractive noise [17] (fluctuations of temperature produce the fluctuations of refractive index) because light beam is traveling inside the corner reflector. However we will show in section V that it is several times smaller than SQL for reflectors manufactured from fused silica. Important that this thermo-refractive noise rapidly decreases with increasing of radius R_b of beam spot as $\sim R_b^{-2}$.

In cavity with CR the thermoelastic noise in the facets remains, but as mentioned above if the reflectors are manufactured from fused silica and the beam spot is large enough (see e.g. [10]) then it is possible to circumvent SQL.

II. THE DISTORTIONS OF MAIN MODE IN FP CAVITY WITH CR

Firstly, we consider FP cavity with two identical perfect corner cube reflectors with three reflecting facets (see fig.1b): i) the corner angles between the facets are exactly equal to $\pi/2$; ii) the top points of the reflectors are located exactly on common optical axis; iii) the "foots" of the reflectors have slight curvatures (shape of a lens surface as shown in fig. 2a) and they are perpendicular to the axis. Then we consider the distortion of mode in this cavity caused by different perturbations.

A. FP resonator with perfect CR

We can consider that each CR consists of reflector with plane foot surface together with spherical lens as shown in fig.2b. The CR produces mirror transformation, i.e. light beam which enters the reflector in point C is transformed into the beam leaving the reflector in point C′. Using Fresnel integral one can obtain the integral equations for calculations of eigenmode distribution:

$$e^{ikL}\int G_0(\vec{r}_1,\vec{r}_2)\,\Phi_2(\vec{r}_2)\,d\vec{r}_2 = \lambda\tilde{\Phi}_1(\vec{r}_1), \qquad (2.1)$$

$$e^{ikL}\int G_0(\vec{r}_1,\vec{r}_2)\,\Phi_1(\vec{r}_2)\,d\vec{r}_1 = \lambda\tilde{\Phi}_2(\vec{r}_2), \qquad (2.2)$$

$$d\vec{r}_1 = dx_1\,dy_1, \quad d\vec{r}_2 = dx_2\,dy_2.$$

Here functions $\Phi_1(\vec{r}_1)$ and $\Phi_2(\vec{r}_2)$ describe distribution of complex field amplitude emitted from imagine flat foot surfaces of reflector 1 (left) and reflector 2 (right) correspondingly just under lenses in planes AA′ and BB′. L is the optical path between reflectors (including path inside the reflector). Evidently phase fronts coincide with planes AA′ and BB′ so that phases of functions Φ_1 and Φ_2 are constants. The notation $\tilde{\Phi}_1(\vec{r}_1)$ means the "mirror" transformation (produced by 3 facets CR) relative to the optical axis[1]:

$$\tilde{\Phi}_1(\vec{r}_1) = \Phi_1(-\vec{r}_1), \qquad \tilde{\Phi}_2(\vec{r}_1) = \tilde{\Phi}_2(-\vec{r}_1)$$

The kernel G^0 is:

$$G_0(\vec{r}_1,\vec{r}_2) = -\frac{i}{2\pi}e^{i\left(\frac{(\vec{r}_1-\vec{r}_2)^2}{2}-h_1(\vec{r}_1)-h_2(\vec{r}_2)\right)}, \qquad (2.3)$$

$$h_1 = \frac{r_1^2}{r_\hbar^2}, \qquad h_2 = \frac{r_2^2}{r_\hbar^2} \qquad (2.4)$$

[1] For 2 facets reflector we have mirror transformation only relatively x coordinate: $\tilde{\Phi}_1(x,y)) = \Phi_1(-x,y)$

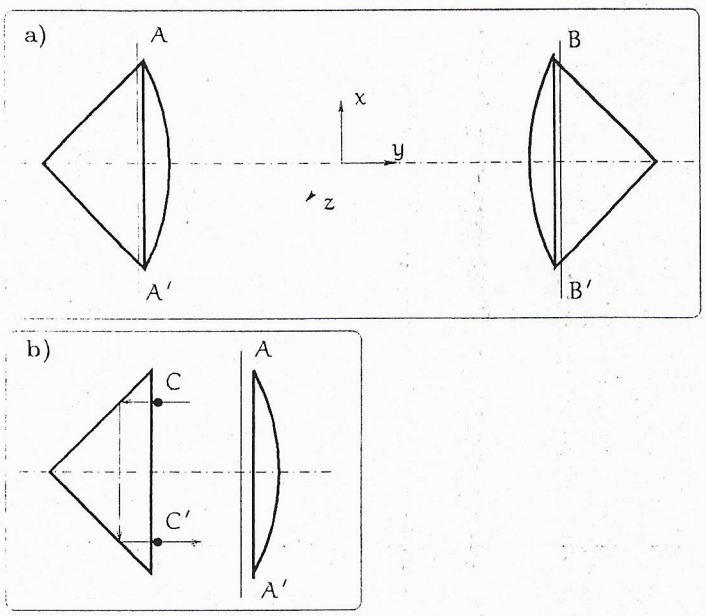

FIG. 2: a). The perfect alignment of CR assembling cavity. b). Each reflector can be regarded as reflector with plane "foot" plus a lens.

Here we use the dimensionless transversal coordinates $\vec{r}_1$ and $\vec{r}_2$ (at planes AA' and BB') which can be expressed in terms of physical coordinates $\vec{R}_1$ and $\vec{R}_2$ as

$$\vec{r}_1 = \frac{\vec{R}_1}{b}, \qquad \vec{r}_2 = \frac{\vec{R}_2}{b}, \qquad b = \sqrt{\frac{L}{k}},$$

where k is wave vector, h_1 and h_2 are additional phase shifts produced by spherical lenses at each reflector foot. It is easy to see that for spherical lenses the set of eigenmodes Φ_1^{mn}, Φ_2^{mn} and their eigenvalues λ_{mn} (below we assume $\lambda_{00} = 1$) of our FP cavity are described by generalized Gauss-Hermite functions:

$$\Phi_1^{mn} = \phi_m(x)\phi_n(y), \tag{2.5}$$

$$\Phi_2^{mn} = (-1)^{-m+n}\Phi_1^{mn} = \tilde{\Phi}_1^{mn} \tag{2.6}$$

$$\phi_m(x) = \frac{1}{\sqrt{r_L}\sqrt{\sqrt{\pi}\,2^m\,m!}} H_m\left(\frac{x}{r_L}\right) \times \tag{2.7}$$

$$\times \exp\left[-i(m+1/2)\psi - \frac{x^2}{2r_L^2}\right],$$

$$\lambda_{mn} = e^{2i(m+n)\psi}, \qquad \psi = \arctan\left(\frac{1}{2r_0^2}\right),$$

$$h_1(r) = h_2(r) = \frac{r^2}{2r_h^2}, \quad 2r_L^2 = 2r_0^2 + \frac{1}{2r_0^2} \tag{2.8}$$

$$2r_h^2 = (2r_0^2)^2 + 1 = 2r_L^2\,2r_0^2. \tag{2.9}$$

Here $H_m(t)$ is the Hermite polynomial of the order m, r_0 and r_L are the radii of beam in the waist and at the lens correspondingly. It is useful to write down the expressions for r_0, r_L, r_h using g-parameter [18] (R^* — is the radius of wave front curvature (in cm) just after the propagation of beam through the lens outside of the reflector):

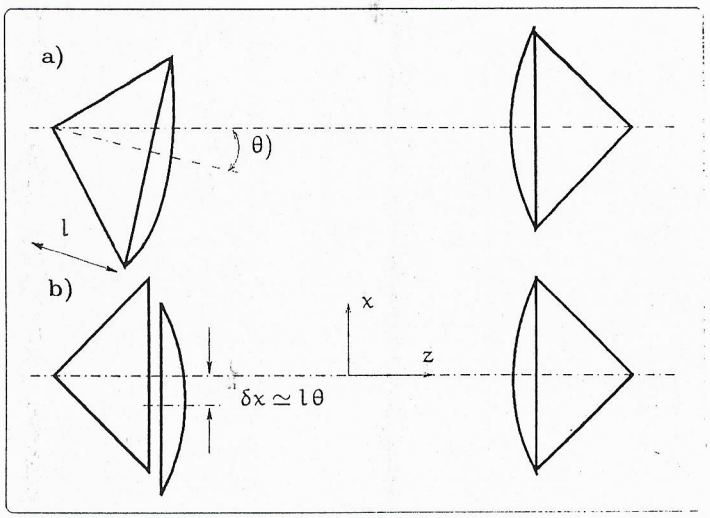

FIG. 3: a). Small tilt of the left CR around its head. b) This tilt is equivalent to untilted reflector and displaced lens.

$$g = 1 - \frac{L}{R^*}, \quad r_0^2 = \frac{1}{2}\sqrt{\frac{1+g}{1-g}}, \tag{2.10}$$

$$r_L^2 = \frac{R_b^2}{b^2} = \frac{1}{\sqrt{1-g^2}}, \quad r_h^2 = \frac{R^*}{L} = \frac{1}{1-g}, \tag{2.11}$$

$$\sin 2\psi = g, \quad \cos 2\psi = \sqrt{1-g^2}. \tag{2.12}$$

We are interested in the main mode $\Phi_1^{00}(x,y)$ of resonator (amplitude distributions of left and right reflectors obviously coincide with each other for the main mode: $\Phi_1^{00}(x,y) = \Phi_2^{00}(x,y)$).

B. Distortion due to the Tilt of CR

Here we consider the main mode $\breve{\Phi}_1^{00}(x,y)$ perturbed due to tilt misalignment shown in fig. 3a. We expand the perturbed main mode into series over the set of unperturbed modes limiting ourselves to the lowest (dipole) approximation:

$$\breve{\Phi}_1^{00}(x_1,y_1) \simeq \Phi_1^{00}(x_1,y_1) - \alpha_1^{tilt}\Phi_1^{10}(x_1,y_1), \tag{2.13}$$

$$\breve{\Phi}_2^{00}(x_2,y_2) \simeq \Phi_2^{00}(x_2,y_2) + \beta_1^{tilt}\Phi_2^{10}(x_2,y_2). \tag{2.14}$$

The tilt of CR around its head through a small angle of θ can be considered as untilted reflector with lens displaced a small distance $\delta x \simeq l\theta$ perpendicular to optical axis (l is the dimensionless distance between the foot and head of CR, it is illustrated in fig. 3b). For this case the perturbations of the main mode can be described by dipole coefficients defined in (2.13, 2.14):

$$\alpha_1^{tilt} \simeq l\theta\,\frac{g(1-g)}{\sqrt{2}(1-g^2)^{3/4}}, \tag{2.15}$$

$$\beta_1^{tilt} \simeq l\theta\,\frac{(1-g)\left[\cot(\psi) - i\right]}{2\sqrt{2}(1-g^2)^{1/4}}, \tag{2.16}$$

$$|\beta_1^{tilt}| \simeq \frac{l\theta}{2}\sqrt[4]{\frac{1-g}{1+g}} \tag{2.17}$$

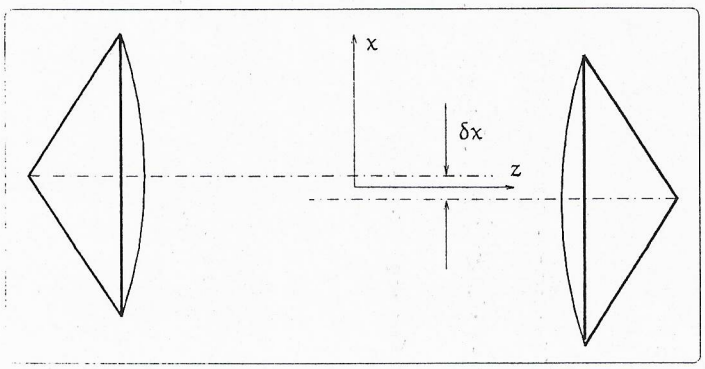

FIG. 4: One CR is displaced relative to another one.

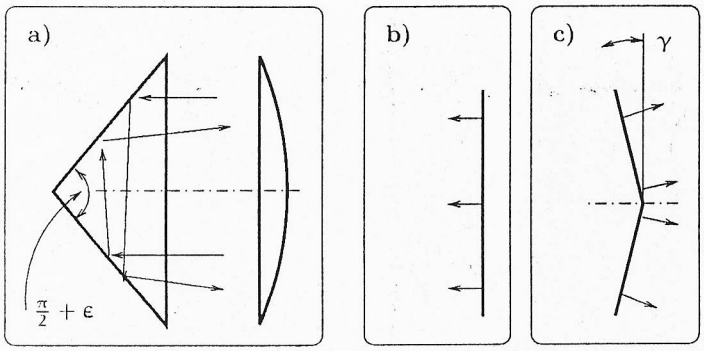

FIG. 5: (a). Expose perturbation: the angle between facets of corner reflector differs from direct angle by a small value of ϵ. It produces the transformation of incident plane wave front (b) into a "broken" front of reflected wave (c).

See details of calculations in Appendix A.

Note that distortion produced by tilt of two facets CR around perpendicular axes (angle $\varkappa$ on fig. 1c) can be described by the same formulas as tilt of spherical mirror.

C. The Distortion due to the Displacement of CR

One CR can be displaced by a small distance δx so that optical axes of reflectors do not coincide with each other as it is shown in fig. 4. For this case the perturbations of the main mode can be described by dipole coefficients defined by formulae (2.13, 2.14). Denoting the dipole coefficients as $\alpha_1^{\rm displ}$ and $\beta_1^{\rm displ}$ one can obtain:

$$\alpha_1^{\rm displ} = \beta_1^{\rm displ} \simeq \frac{-\delta x}{2\sqrt{2}}\left(\frac{-2ig}{\sqrt[4]{1-g^2}} + \sqrt[4]{1-g^2}\right) \qquad (2.18)$$

See details of calculations in Appendix B.

D. The Distortion of Expose Angle

Here we consider the case when, for example the left reflector (2-hedral prism shown in fig. 1c) has a non-perfect perpendicular facets, so that expose angle between them differs from $\pi/2$ by a small angle of ϵ (fig. 5a). Then the plane front of incident wave after reflection from the reflector is transformed into a broken surface consisting of two plane parts declined to the incident wave front by an angle of $\gamma = 2\epsilon$ as shown in fig. 5b,c.

This statement is also correct for tri-hedral reflectors (shown in fig. 1b) with the exception of numerical factor: if only one facet is declined by angle of ϵ from the normal position (and other two facets are non-perturbed) the angle γ will be equal to $\gamma = 2\epsilon\sqrt{2/3}$.

Again we can expand the perturbed main mode over the set of unperturbed modes of ideal cavity keeping only the lowest first-order non-vanishing term of expansion:

$$\check{\Phi}_1^{00}(x_1, y_1) \simeq \Phi_1^{00}(x_1, y_1) + \alpha_2^{\rm expose}\Phi_1^{20}(x_1, y_1), \quad (2.19)$$

$$\check{\Phi}_2^{00}(x_2, y_2) \simeq \Phi_2^{00}(x_2, y_2) + \beta_2^{\rm expose}\Phi_2^{20}(x_2, y_2) \quad (2.20)$$

(due to the symmetry of this kind perturbation the dipole term is null). Calculation gives the following value for α_2:

$$\alpha_2^{\rm expose} \simeq \frac{i\gamma L}{4\sqrt{2}\pi b\sqrt[4]{1-g^2}} \times \frac{\left(g + i\sqrt{1-g^2}\right)^2}{i\,g\,\sqrt{1-g^2}} \qquad (2.21)$$

$$|\alpha_2^{\rm expose}| = |\beta_2^{\rm expose}| \simeq \frac{L\gamma}{4\sqrt{2}\pi\, b\, g(1-g^2)^{3/4}} \qquad (2.22)$$

See details in Appendix C.

III. COMPARISON OF FP CAVITIES WITH CR AND WITH SPHERICAL MIRRORS

Recall that uncontrollable perturbations of the mode produce additional noise: in laser interferometer gravitational antenna the signal at dark port will contain additional noise with power proportional to the square of distortion coefficients $\sim |\alpha|^2, |\beta|^2$. In this section we compare numerically the distortion of the main mode in traditional FP cavity with spherical mirrors (SM cavity) with FP cavity assembled by CR (CR cavity).

The distortion of the main mode in SM cavity caused by small displacement and tilt of one mirror can be also described by coefficients α_1 of expansion (2.13)[20, 21]:

$$\alpha_1^{\rm tilt,\ Sph} = \frac{l}{\sqrt{2}(1-g^2)^{3/4}}\left(\frac{\theta L}{b}\right), \qquad (3.1)$$

$$\alpha_1^{\rm displ,\ Sph} = \left(\frac{(1-g)^{1/4}}{\sqrt{2}(1+g)^{3/4}}\right)\delta x \qquad (3.2)$$

For estimates for both SM and CR cavity we use the parameters of cavity proposed for Advanced LIGO [20]:

$$r_L = 6/2.6 \simeq 2.3, \quad g = 0.982. \qquad (3.3)$$

These parameters correspond to the radius of laser beam R_b at the reflector surface of about $R_b \simeq 6$ cm. Assuming additionally that dimension length l^* from foot to top is equal to $l^* = 20$ cm, i.e.

$$l = \frac{20\,\text{cm}}{b} \simeq 7.7,$$

and dimension displacement $\delta x^* = b\,\delta x$ we obtain the following estimates for SM cavity:

$$\alpha_1^{\rm tilt,\ SM} = 0.013\left(\frac{\theta}{10^{-8}}\right), \qquad (3.4)$$

$$\alpha_1^{\rm disp,\ SM} = 0.0059\left(\frac{\delta x^*}{0.1\ \text{cm}}\right) \qquad (3.5)$$

and for CR cavity:

$$\alpha_1^{\text{tilt, CR}} = 1.2 \times 10^{-7} \left(\frac{\theta}{10^{-8}} \right), \qquad (3.6)$$

$$\alpha_1^{\text{displ, CR}} = 0.06 \left(\frac{\delta x^*}{0.1 \text{ cm}} \right), \qquad (3.7)$$

$$\alpha_2^{\text{expose}} = 0.11 \left(\frac{\gamma}{10^{-6}} \right). \qquad (3.8)$$

We see that CR cavity is substantially more stable to tilt and less stable to displacement than SM cavity. However, the total requirements for SM cavity looks more tough if one compares the estimates (3.4 and 3.7). Indeed to keep control of tilt in SM cavity with accuracy $\theta \simeq 10^{-8}$ rad (see (3.4)) one has to operate the positioning system with accuracy about $lb\,\theta \simeq 2 \times 10^{-6}$ cm. But the same level of displacement distortion in CR cavity (see (3.7)) one can obtain by displacement control with much lower accuracy: ≤ 1 mm only (!).

The requirement for an expose angle in CR cavity looks also acceptable: for accuracy of manufacturing $\epsilon \simeq 3 \times 10^{-7}$ (commercially available prisms have $\epsilon \simeq \pm 1 \times 10^{-5}$) and hence $\gamma = 2\epsilon\sqrt{2/3} \simeq 4.9 \times 10^{-7}$ we have to take into account that three angles between facets (increasing factor $\sqrt{3}$) in each of two tri-hedral reflector (one more increasing factor $\sqrt{2}$) may be independently perturbed (so the total increasing factor is equal to $\sqrt{3} \times \sqrt{2} = \sqrt{6}$):

$$\sqrt{\sum \left(\alpha_{2,\,i}^{\text{expose}}\right)^2} \simeq \sqrt{6}\,\alpha_2^{\text{expose}} \simeq 0.13$$

Optical inhomogeneity is one more source of perturbation which is specific to CR: the refraction index of fused silica (which CR is manufactured from) changes over the value of $\delta n \simeq 2 \times 10^{-7}$ along the length $\Delta l \simeq 10$ cm [22]. To estimate negative influence of this effect we can consider the model task using the fact that distance scale Δl of refraction index perturbation is about the dimension bl of the reflector. Let one half of corner reflector has a perturbed refraction index $n + \Delta n(x)$ which depends on a transversal coordinate x only:

$$\Delta n(x) = \begin{cases} \Delta n = -\delta n \left(1 - \frac{x}{l}\right) & \text{if} \quad x > 0, \\ \Delta n = 0 & \text{if} \quad x \leq 0 \end{cases} \qquad (3.9)$$

In this case the beam after reflection from such a reflector will have a broken wave front as shown in fig. 5c with angle

$$\gamma = \frac{\delta n}{4n} \qquad (3.10)$$

Hence one can estimate the value of perturbation due to inhomogeneity using formula (2.22). It is obvious that for perturbation with another dependence of Δn on space coordinates the formula (3.10) must change this estimate by the factor of about unity or slightly larger. So for estimates we use the 4 times greater value of γ than (3.10). In that case for two reflector with independently perturbed refraction index (factor $\sqrt{2}$) we obtain:

$$\gamma = \frac{\sqrt{2}\,\delta n}{n} \simeq 2 \times 10^{-7}, \quad \alpha_2^{\text{inhomo}} \simeq 0.011 \qquad (3.11)$$

The two last kinds of perturbations (expose angle and inhomogeneity) depend only on manufacturing procedure and there is a hope they can be decreased due to the improvement of manufacturing culture.

IV. THE OPTICAL LOSSES

The loss coefficient for CR cavity must be small — about 10 ppm. We consider the following sources of losses.

Fundamental losses on edge are produced by diffraction on edge where two facets meet. Qualitatively it can be described as two surface waves outside CR (bounded with waves inside due to complete internal reflection) meet at edge producing diffractional scattering (we acknowledge to F.Ya.Fhalili pointed out the existtence of this kind losses).

To our best knowledge nobody performed rigorous analysis of this problem. So we propose the consideration to estimate this effect: (a) using the formulas for complex coefficient of reflection for plane wave from plane infinite boundary between two media for the case of internal reflection (see e.g. [23]) one can construct the solution *inside* CR; (b) using the boundary condition one can obtain the fields along *outside* surface of CR; (c) applying Green's formula one can calculate the radiation field in far wave zone and total diffractional power. The most vulnerable for critics item of this consideration is (a) — applying the formulas for infinite boundary to corner configuration.

We apply this consideration for the case of incident wave polarized along edge of CR of "roof" type (fig. 1c). For this particular case (with obvious assumption that magnetic permittivity $\mu = 1$) the all field components of constructed solution are smooth inside CR and on outside surface CR. Our calculation gives the following loss coefficient:

$$(1 - R)_d \simeq \frac{0.4\lambda}{R_b} \simeq 0.7 \times 10^{-5} \qquad (4.1)$$

where λ is the optical wavelength, (see details in Appendix D).

Note that our consideration of incident wave polarized perpendicular to the edge of CR allows to construct smooth solution inside CR but this solution on the outside surface will have break of components of electrical fields at the edge. Thus to get a reliable confirmation of the approximatetive estimate (4.1) it is necessary either to find a rigorous analytical solution of this problem or to perform straightforward numerical calculation.

The losses on non-perfect edge is produced by scattering of the plane optical wave on the non-perfect "ridges" where two facets meet. The edge of facets intersection with uncontrollable width of $\Delta s \leq 0.5$ μm will produce optical losses which can be roughly estimated as following:

$$(1 - R)_{\text{non-perfect}} \leq \frac{\Delta s}{R_b} \simeq 0.8 \times 10^{-5}$$

In other words it satisfies our initial condition to obtain $\tau_{FP}^* \simeq 1$s.

Optical losses of material. Internal optical losses in purified fused silica at the level $\gamma_{\text{loss}} \simeq 0.5$ ppm/cm [19] give the loss coefficient about

$$(1 - R)_{\text{opt.loss}} \simeq \gamma_{\text{loss}} 2bl \simeq 0.8 \times 10^{-5}$$

Losses in anti reflective coating. As we mentioned in Introduction it will be necessary to use anti reflective coating on the bottom surfaces of CR. Calculations which we omit here shows that to keep the value of $(1 - R)$ at the level $\sim 10^{-5}$ it is sufficient to use 2-4 anti reflective layers of coating.

V. THERMO-REFRACTIVE NOISE

The origin of thermo-refractive noise is thermodynamic (TD) fluctuations of temperature which produce fluctuations of phase of light traveling inside the CR through dependence of refractive index n on temperature T: $\beta = dn/dT \neq 0$ [17]. One can estimate TD temperature fluctuations using the model of infinite layer with width l_c ($0 \le z \le l_c$). We additionally assume that layer is in vacuum and its both surfaces are thermally isolated (thermal radiation in accordance with Stefan-Boltzmann law is so small that this assumption is quite correct). If light (Gaussian beam) with radius R_b travels through the layer perpendicular to its surface the fluctuations φ of light phase during time τ will be defined by TD temperature fluctuations u averaged over the cylinder $\pi R_b^2 l_c$:

$$\varphi = k l_c \beta \sqrt{\langle \bar{u}^2 \rangle_\tau}, \quad k = \frac{2\pi}{\lambda}. \tag{5.1}$$

Subscript τ means that we are interested in *variation* of temperature during observation time τ.

The total variation of TD temperature fluctuations is equal to

$$\langle \bar{u}^2 \rangle = \frac{k_B T^2}{\rho C \pi R_b^2 l_c}$$

where k_B is the Boltzmann constant, ρ is density, and C is the specific heat capacity. Then the variation of temperature over the small time τ (adiabatic approximation) must be about $\langle \bar{u}^2 \rangle_\tau \simeq \langle \bar{u}^2 \rangle \times \tau/\tau^*$ where $\tau^* = \rho C R_b^2/\kappa$ is thermal relaxation time of our cylinder through lateral surface (base surfaces of cylinder are thermo isolated), κ is thermal conductivity. Here we assume that $\tau \ll \tau^*$. This result can be rewritten in form

$$\langle \bar{u}^2 \rangle_\tau = \frac{k_B T^2}{\rho C \pi R_b^2 l_c} \times \left(\frac{r_T^2}{R_b^2} \right), \quad r_T = \sqrt{\frac{\kappa \tau}{\rho C}} \ll R_b,\ l$$

where r_T is thermal diffusive length for the time τ.

Equating $\langle \bar{u}^2 \rangle_\tau \simeq S_{\bar{u}}(\omega)\, \Delta\omega$ we can obtain the estimate for spectral density $S_{\bar{u}}(\omega)$ of averaged temperature putting $\omega \simeq \Delta\omega \simeq 1/\tau$.

The accurate expressions for these spectral densities $S_u(\omega)$ and $S_\varphi(\omega)$ of temperature fluctuations and phase fluctuations correspondingly are the following

$$S_{\bar{u}}(\omega) \simeq \frac{4 k_B T^2 \kappa}{(\rho C)^2 l_c} \frac{1}{\pi R_b^4 \omega^2}, \tag{5.2}$$

$$S_\varphi(\omega) \simeq \frac{4 \beta^2 k^2 l_c k_B T^2 \kappa}{(\rho C)^2} \frac{1}{\pi R_b^4 \omega^2} \tag{5.3}$$

for adiabatic case, i.e. for $\omega \gg \frac{\kappa R_b^2}{\rho C}$.

One can easy check that our estimate differs from accurate expression (5.2) for $S_{\bar{u}}(\omega)$ only by the factor of about unity. In Appendix E we present derivation of general expression for adiabatic and non-adiabatic cases.

The formulae (5.2, 5.3) allows to recalculate thermo-refractive fluctuations into the fluctuations of dimensionless metric h (which usually describes the sensitivity of laser gravitational antennae): $h = \varphi/(kL)$, where L is cavity length. It is useful to estimate its spectral density $S_h(\omega)$ for parameters of laser gravitational antenna (advanced LIGO) presented in Appendix F and $l_c = 10$ cm:

$$\sqrt{S_h(\omega)} \simeq 0.5 \times 10^{-24}\ \mathrm{Hz}^{-1/2}. \tag{5.4}$$

It is about 4 times smaller than the sensitivity of Standard Quantum Limit (1.1) which is planned to achieve in Advanced LIGO [19]. Important that this thermo-refractive noise rapidly decreases with increase of beam radius: $\sqrt{S_h(\omega)} \sim R_b^{-2}$. Thus the using so called "mesa-shaped" beams [20, 21] (having flat distribution in the center and fall to zero more quickly than Gaussian distribution at the edges) with larger radius will allow to decrease thermo-refractive noise by several times. For example using the 45×45 cm^2 foot of CR and $R_b = 10$ cm with mesa shape distribution of the intensity of light in the beam one may expect the gain of sensitivity for $\sqrt{S_h(\omega)}$ approximately one order better than $\sqrt{S_h^{SQL}(\omega)}$.

VI. CONCLUSION

The presented analysis of FP cavity with two CR (instead of mirrors) has to be regarded as an example of cavity in which thermoelastic noise in the coating may be substantially decreased and which permits to circumvent substantially the SQL of sensitivity and also to have $(1-R) \approx 10^{-5}$.

We have shown that CR cavity is considerably more stable than cavity with spherical mirrors relative to tilt and displacement distortion. The distortion due to expose angle of CR is not so small but it depends only on manufacturing procedure, and there is a hope to decrease it due to improvement of manufacturing culture.

There does exist another argument in favor of using CR in FP resonators. The very recent measurements performed by LIGO collaborators from University of Glasgow, Stanford University, Iowa State University, Syracuse University and LIGO Lab have shown that multi-layer coating also decreases the quality factors of mirrors internal modes [24]. This effect may substantially increase the Brownian component of the noise in the mirror itself and thus decrease the sensitivity of LIGO antennae (see details on Brownian moise in coating in [25–30]).

At the same time it is likely that there does exist other version of cavity free from thermoelastic noise in coating, probably more easy to implement which evidently deserves similar in-depth analysis. One of the "candidates" is a cavity with unusual reflective coating: each layer of it has to have the same small value of thermal expansion as fused silica. Unfortunately the technology which may provide it is not yet invented.

In the above analysis we have limited ourselves to the calculations of the cavity properties itselves and did not discuss the coupling of cavity with pumping laser and readout system. This analysis has to be done especially because the readout system may be an intra-cavity one [8] and because special attention has to be paid to the possible specific deformation of the main mode distribution in FP cavity with CR. One of several possible ways to realize the coupling of the mode with pumping source may be based on the existence of the evanescent optical field "outside" the surface of the facets. In this case it will be evidently necessary to use very thin dielectric grating on the surface of the facet.

We have not also discuss the polarization characteristics of CR. For example it is known that the phase shift of wave reflected from plane surface depends on polarization [23]) and hence the FP cavity with 2-facets CR will have slightly different eigen frequencies for waves with polarization along and perpendicular to edge of CR. The additional problem to be analyzed is the polarization characteristics of 3-facets CR.

It seems that the CR cavity for Advanced LIGO have to be used not for modes with Gaussian distribution of power over the cross section but for so called "mesa-shaped" [20, 21] mode with flat distribution in the center and fall to zero more quickly than Gaussian distribution at the edges. For "mesa-shaped" modes the profile of "lenses" (h_1 and h_2 in 2.3) on the foot of the corner reflector must have special dependence on radius calculated in [20, 21].

It is worth noting that the discussed in this paper features of CR cavity may be useful not only for the gravitational wave antennae but also in other high resolution spectroscopic experiments where the low level of optical eigenmode fluctuations is important.

Acknowledgments

We are very grateful to A. S. Ilinsky and F. Ya. Khalili for very fruitful notes and discussions. This work was supported by LIGO team from Caltech and in part by NSF and Caltech grant PHY0098715, by Russian Ministry of Industry and Science contracts # 40.02.1.1.1.1137 and # 40.700.12.0086, and by Russian Foundation of Basic Researches grant #03-02-16975-a.

APPENDIX A: TILT OF CORNER REFLECTION

The tilt of one reflector through angle θ (see fig.3a) can be considered as displacement of lens on distance $\delta x \simeq l\theta$ (see fig.3b) perpendicular to axis. Then the set of integral equations (2.1, 2) for eigen mode have the same form with replacing kernel $G_0 \to G_1$:

$$G_1 \simeq G_0 \left(1 - \frac{ix_1\,\delta x}{r_h^2}\right). \tag{A1}$$

The perturbed main modes $\breve{\Phi}_1^{00}(x_1, y_1)$, $\breve{\Phi}_2^{00}(x_2, y_2)$ we find as expansion into series over eigen functions of resonator with perfectly positioned reflectors:

$$\breve{\Phi}_1^{00}(x_1, y_1) = \phi_0(y_1) \sum_m (-1)^m \alpha_m \phi_m(x_1), \tag{A2}$$

$$\breve{\Phi}_2^{00}(x_2, y_2) = \phi_0(y_2) \sum_m \beta_m \phi_m(x_2). \tag{A3}$$

After substitution these expansions into set (2.1, 2) replacing kernel $G_0 \to G_1$ we obtain:

$$\sum_m \lambda_m (-1)^m \alpha_m \phi_m(x_2) - \tag{A4}$$
$$- e^{ikL} \int G_0(\vec{r}_1, \vec{r}_2) \left(\frac{ix_1\,\delta x}{r_h^2}\right) \times$$
$$\times \sum_m (-1)^m \alpha_m \phi_m(x_1)\, dx_1 =$$
$$= \Lambda \sum_m (-1)^m \beta_m \phi_m(x_2),$$

$$\sum_m \lambda_m \beta_m \phi_m(x_1) - e^{ikL} \int G_0(\vec{r}_1, \vec{r}_2) \times \tag{A5}$$
$$\times \left(\frac{ix_1\,\delta x}{r_h^2}\right) \sum_m \beta_m \phi_m(x_2)\, dx_2 =$$
$$= \Lambda \sum_m \alpha_m \phi_m(x_1)$$

Here Λ is eigen value of perturbed main mode.

After multiplying equation (A4) by $\phi_{m_0}(x_2)$ and integrating we obtain:

$$\Lambda \beta_{m_0} = \lambda_{m_0,0} \alpha_{m_0} + I_{m_0}, \tag{A6}$$
$$I_{m_0,0} = \frac{i\,\delta x\, r_L}{\sqrt{2}\, r_h^2} \lambda_{m_0,0} \times$$
$$\times \left(\alpha_{m_0-1}\sqrt{m_0} + \alpha_{m_0+1}\sqrt{m_0+1}\right)$$

After multiplying equation (A5) by $\phi_{m_0}(x_1)$ and integrating we obtain:

$$\Lambda m_0 \alpha_{m_0} = \lambda_{m_0,0} \beta_{m_0} + J_{m_0,0}, \tag{A7}$$
$$J_{m_0,0} = \frac{i\delta x\, r_L}{\sqrt{2}\, r_h^2} \left(\lambda_{m_0-1}\, \beta_{m_0-1} \sqrt{m_0} + \right.$$
$$\left. \lambda_{m_0+1}\, \beta_{m_0+1} \sqrt{m_0+1}\right)$$

Now we can rewrite equations (A6,A7) for different m_0 taking in mind that α_0, $\beta_0 \simeq 1$, $\alpha_1 \simeq \beta_1 = \mathcal{O}(\delta x)$, $\alpha_2 \simeq \beta_2 = \mathcal{O}(\delta x^2)$, ...:

$$m_0 = 0, \quad \lambda_0 \alpha_0 + \frac{i\delta x\, r_L}{\sqrt{2}\, r_h^2} \lambda_0 \alpha_1 = \Lambda \beta_0, \tag{A8}$$

$$\Lambda \alpha_0 = \lambda_0 \beta_0 + \frac{i\delta x\, r_L}{\sqrt{2}\, r_h^2} \lambda_1 \beta_1, \tag{A9}$$

$$\Rightarrow \alpha_0 \simeq \beta_0 \simeq 1, \quad \Lambda = \lambda_0 + \mathcal{O}(\delta x^2), \tag{A10}$$

$$m_0 = 1, \quad \lambda_1 \alpha_1 - \Lambda \beta_1 \simeq \frac{-i\delta x\, r_L}{\sqrt{2}\, r_h^2} \lambda_1, \tag{A11}$$

$$-\Lambda \alpha_1 + \lambda_1 \beta_1 \simeq \frac{-i\delta x\, r_L}{\sqrt{2}\, r_h^2} \lambda_0, \tag{A12}$$

$$\Rightarrow \alpha_1 \simeq \frac{-i\delta x\, r_L (\lambda_1^2 + \lambda_0^2)}{\sqrt{2}\, r_h^2 (\lambda_1^2 - \lambda_0^2)}, \tag{A13}$$

$$\Rightarrow \beta_1 \simeq \frac{-i\delta x\, r_L\, \lambda_1}{\sqrt{2}\, r_h^2 (\lambda_1 - \lambda_0)}, \tag{A14}$$

$$m_0 = 2, \quad \lambda_2\alpha_2 - \Lambda\beta_2 \simeq \frac{-i\delta x\, r_L}{\sqrt{2}\, r_h^2}\lambda_2\sqrt{2}\alpha_1, \tag{A15}$$

$$-\Lambda\alpha_2 + \lambda_2\beta_2 \simeq \frac{-i\delta x\, r_L}{\sqrt{2}\, r_h^2}\sqrt{2}\lambda_1\beta_1, \tag{A16}$$

$$\Rightarrow \alpha_2 \simeq \frac{-i\delta x\, r_L}{r_h^2}\frac{\left(\lambda_2^2\alpha_1 + \lambda_1\lambda_0\beta_1\right)}{\left(\lambda_2^2 - \lambda_0^2\right)}, \tag{A17}$$

$$\Rightarrow \beta_2 \simeq \frac{-i\delta x\, r_L}{r_h^2}\frac{\lambda_2\left(\lambda_0\alpha_1 + \lambda_1\beta_1\right)}{\left(\lambda_2^2 - \lambda_0^2\right)}, \tag{A18}$$

Rewriting values α_1 and β_1 using g-parameter (2.10 – 2.12) one can obtain formulas (2.15 – 2.17).

APPENDIX B: DISPLACEMENT OF CR

Let the right corner is displaced by value δx in transversal direction (see fig. 4). Then the integral equations for perturbed eigen mode is the following

$$e^{ikL}\int G_1(x_1,y_1,x_2,y_2)\,\breve{\Phi}_1(x_1,y_1)\,dx_1\,dy_1 = \tag{B1}$$

$$= \Lambda\,\breve{\Phi}_2(\delta x - x_2, -y_2), \tag{B2}$$

$$e^{ikL}\int G_1(x_1,y_1,x_2,y_2)\,\breve{\Phi}_2(x_2,y_2)\,dx_2\,dy_2 = \tag{B3}$$

$$= \Lambda\,\breve{\Phi}_1(-\delta x - x_1, -y_1), \tag{B4}$$

$$\breve{\Phi}_1(-\delta x - x_1, -y_1) \simeq \breve{\Phi}_1(-x_1,-y_1) - \tag{B5}$$

$$-\delta x\,\partial_{x_1}\breve{\Phi}_1(-x_1-y_1),$$

$$\breve{\Phi}_2(\delta x - x_2, -y_2) \simeq \breve{\Phi}_2(-x_2,-y_2) + \tag{B6}$$

$$+\delta x\,\partial_{x_2}\breve{\Phi}_2(-x_2-y_2),$$

$$G_1(x_1,y_1,x_2,y_2) \simeq G_0(x_1,y_1,x_2,y_2)\times \tag{B7}$$

$$\times\left(1 - i\left[\delta h_1 + \delta h_2\right]\right),$$

$$\delta h_1 \simeq \frac{x_1\delta x}{2r_h^2}, \quad \delta h_2 \simeq \frac{-x_2\delta x}{2r_h^2}. \tag{B8}$$

We find perturbed main mode distributions $\breve{\Phi}_1^{00}(x_1,y_1)$, $\breve{\Phi}_2^{00}(x_2,y_2)$ as expansion into series over eigen functions of resonator with perfectly positioned reflectors:

$$\Phi_1^{00}(x_1,y_1) = \phi_0(y_1)\sum_m (-1)^m\alpha_m\phi_m(x_1) \tag{B9}$$

$$\Phi_2^{00}(x_2,y_2) = \phi_0(y_2)\sum_m \beta_m\phi_m(x_2). \tag{B10}$$

After substitution these expansions into (B1 - B7) we obtain:

$$\sum_m \lambda_{m,0}(-1)^m\alpha_m\phi_m(x_2) - e^{ikL}\int G_0(\vec{r}_1,\vec{r}_2)\times$$

$$\times\left(\frac{i(x_1-x_2)\delta x}{2r_h^2}\right)\sum_m(-1)^m\alpha_m\phi_m(x_1)\,dx_1 =$$

$$=\Lambda\sum_m(-1)^m\beta_m\phi_m(x_2) + \tag{B11}$$

$$+\Lambda\delta x\sum_m(-1)^m\beta_m\left(\partial_{x_2}\phi_m(x_2)\right),$$

$$\sum_m \lambda_{m,0}\beta_m\phi_m(x_1) - e^{ikL}\int G_0(\vec{r}_1,\vec{r}_2)\times \tag{B12}$$

$$\times\left(\frac{i(x_1-x_2)\delta x}{2r_h^2}\right)\sum_m\beta_m\phi_m(x_2)\,dx_2 =$$

$$=\Lambda\sum_m\alpha_m\phi_m(x_1) - \Lambda\delta x\sum_m\alpha_m\left(\partial_{x_1}\phi_m(x_1)\right),$$

After multiplying equation (B11) by $\phi_{m_0}(x_2)$ and integrating we obtain:

$$\lambda_{m_0,0}\alpha_{m_0,0} + I_{m_0,0} = \Lambda\,\beta_{m_0,0} + J_{p_0,0}, \tag{B13}$$

$$I_{m_0,0} = \frac{i\delta x\, r_l}{2\sqrt{2}\, r_h^2}\left(\left[\lambda_{m_0,0} - \lambda_{m_0-1,0}\right]\sqrt{m_0}\alpha_{m_0-1} + \right.$$

$$\left. +\left[\lambda_{m_0,0} - \lambda_{m_0+1,0}\right]\sqrt{m_0+1}\alpha_{m_0+1}\right),$$

$$J_{m_0,0} = -\frac{\Lambda\,\delta x}{r_L}\left(\beta_{m_0+1}\sqrt{\frac{m_0+1}{2}} - \beta_{m_0-1}\sqrt{\frac{m_0}{2}}\right).$$

After multiplying equation (B12) by $\phi_{m_0}(x_1)$ and integrating we obtain:

$$\lambda_{m_0,0}\beta_{m_0,0} + I'_{m_0,0} = \Lambda\,\alpha_{m_0,0} + J'_{p_0,0}, \tag{B14}$$

$$I'_{m_0,0} = \frac{i\delta x\, r_l}{2\sqrt{2}\, r_h^2}\left(\left[\lambda_{m_0,0} - \lambda_{m_0-1,0}\right]\sqrt{m_0}\alpha_{m_0-1} + \right.$$

$$\left. +\left[\lambda_{m_0,0} - \lambda_{m_0+1,0}\right]\sqrt{m_0+1}\alpha_{m_0-1}\right),$$

$$J'_{m_0,0} = \frac{-\Lambda\,\delta x}{\sqrt{2}\, r_L}\left(\alpha_{m_0+1}\sqrt{m_0+1} - \alpha_{m_0-1}\sqrt{m_0}\right).$$

Here we use the rule: coefficients $\alpha_m = 0$ and $\beta_m = 0$ if $m < 0$.

Substituting $I_{m_0,0}$ and $J_{m_0,0}$ into (B13) and substituting $I'_{m_0,0}$ and $J'_{m_0,0}$ into (B14) we obtain two equations. They may be transformed from one to other by replacement $\alpha_m \to \beta_m$ and vice versa $\beta_m \to \alpha_m$. So assuming that $\alpha_m = \beta_m$ we can solve only one equation:

$$\lambda_{m_0,0}\alpha_{m_0} + \frac{i\delta x\, r_L}{2\sqrt{2}\, r_h^2}\times \tag{B15}$$

$$\times\left(\left[\lambda_{m_0,0} - \lambda_{m_0-1,0}\right]\sqrt{m_0}\alpha_{m_0-1} + \right.$$

$$\left. +\left[\lambda_{m_0,0} - \lambda_{m_0+1,0}\right]\sqrt{m_0+1}\alpha_{m_0+1}\right)$$

$$=\Lambda\,\alpha_{m_0} - \frac{\Lambda\,\delta x}{\sqrt{2}\, r_L}\left(\alpha_{m_0+1}\sqrt{m_0+1} - \alpha_{m_0-1}\sqrt{m_0}\right),$$

We assume that $\lambda_{0,0} = 1$, $\Lambda = \lambda_{0,0} + \Delta = 1 + \Delta$, $\alpha_0 \simeq 1$, $\alpha_1 \sim \delta x$, $\alpha_2 \sim \delta x^2$, ... Putting $m_0 = 0$ in (B15) we obtain $\Delta \sim \delta x^2$. And putting $m_0 = 1$ in (B15) we find

$$\alpha_1 \simeq -\alpha_0\frac{\delta x}{\sqrt{2}\, r_L}\left(\frac{ir_L^2}{2r_h^2} + \frac{1}{1-\lambda_{1,0}}\right) \tag{B16}$$

Using (2.10 – 2.12) one can rewrite this formula in form (2.18).

APPENDIX C: EXPOSE PERTURBATION OF CR

For this case the equations for eigen modes calculations are the following in this section we do not mark by ˘ distri-

TABLE I: Numerical values of coefficients $F_{m_0,m}$ for low indices

	$m=0$	$m=2$	$m=4$	$m=6$
$m_0=0$	$1/\sqrt{\pi}$	$1/\sqrt{2\pi}$	$-1/(2\sqrt{6\pi})$	$1/(4\sqrt{5\pi})$

bution function of perturbed mode:

$$e^{ikL}\int G_0(\vec{r}_1,\vec{r}_2)\,\Phi_2(\vec{r}_2)\,d\vec{r}_2 \simeq \tag{C1}$$
$$\simeq \Lambda\tilde{\Phi}_1(\vec{r}_1)\left(1-ib\gamma k|x_1|\right),$$
$$e^{ikL}\int G_0(\vec{r}_1,\vec{r}_2)\,\Phi_1(\vec{r}_2)\,d\vec{r}_2 =\simeq \Lambda\tilde{\Phi}_2(\vec{r}_2).$$

We find the solutions as expansion

$$\Phi_1(x_1,y_1)=\phi_0(y_1)\sum_m(-1)^m\alpha_m\phi_m(x_1) \tag{C2}$$

$$\Phi_2(x_2,y_2)=\phi_0(y_2)\sum_m\beta_m\phi_m(x_2). \tag{C3}$$

Substituting them into equations (C1, C2) we obtain

$$\sum_m\lambda_{m,0}\beta_m\phi_m(x_1)= \tag{C4}$$
$$=\Lambda\sum_m\alpha_m\phi_m(x_1)\left(1-ib\gamma k|x_1|\right),$$
$$\sum_m\lambda_{m,0}(-1)^m\alpha_m\phi_m(x_2)=\Lambda\sum_m(-1)^m\beta_m\phi_m(x_2) \tag{C5}$$

From last equation we obtain

$$\beta_m=\frac{\lambda_{m,0}}{\Lambda}\alpha_m$$

and substitute it into (C4). After multiplying obtained equation by $\phi_{m_0}(x_1)$ and integrating over dx_1 we get:

$$\lambda^2_{m,0}\alpha_{m_0}=\Lambda^2\alpha_{m_0}-ib\gamma\Lambda^2 kr_L\sum_m\alpha_m F_{m_0,m}, \tag{C6}$$

$$F_{m_0,m}=\int_{-\infty}^{\infty}|x|\,\phi_m(x)\,\phi_{m_0}(x)\,dx \tag{C7}$$

We have tabulated coefficients F_{m,m_0} — result is presented in Table I.

Assuming that $\lambda_{0,0}=1$ and $\alpha_0\simeq 1$, α_1, $\alpha_2,\cdots\ll 1$ we see that this system can be divided by two independent subsystems: one for odd indices and another one — for even indices. Odd indices can be put zero and for even indices we have

$$\Lambda^2\simeq 1+\frac{iL\gamma r_L}{b\sqrt{\pi}}, \tag{C8}$$

$$\alpha_2\simeq\frac{iL\gamma kr_L}{\sqrt{2\pi}\,b\left(1-e^{-8i\psi}\right)}, \tag{C9}$$

$$\alpha_4\simeq\frac{iL\gamma kr_L}{2\sqrt{6\pi}\,b\left(1-e^{-16i\psi}\right)}, \tag{C10}$$

We see that all coefficients α_2, $\alpha_4,\cdots\sim\gamma$, i.e. they have the same order over γ. However the convergence seems to take place due to decreasing the coefficients $F_{m0,0}\sim 1/m_0^{5/4}$ with $m_0\to\infty$.

These expressions can be rewritten using g-parameter in form (2.21, 2.22).

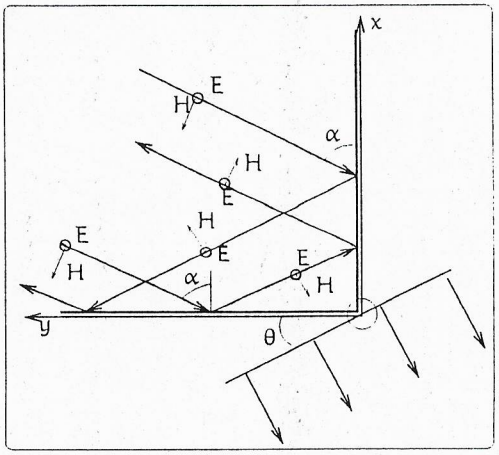

FIG. 6: Plane wave traveling and reflecting from dielectric corner reflector with angle between facets $\pi/2$. The axis z is directed upward and perpendicular to plane of figure. Vector E is directed along z-axis.

APPENDIX D: DIFFRACTIONAL LOSSES ON EDGE

Here we write down the calculations to obtain estimate (4.1). We consider the monochromatic plane wave polarized along z-axis traveling and reflecting from dielectric CR with angle between facets $\pi/2$ (see fig. 6). Incident wave:

$$E_{z\,inc}=E_0\exp\left(-i\omega t-ikn\sin\alpha\,x-ikn\cos\alpha\,y\right),$$
$$\vec{H}=\left[\vec{k}\,\vec{E}\right],\quad \mu=1,$$

Below I drop the multiplier $e^{-i\omega t}$. Condition of internal reflection is fulfilled on both facets: $n\cos\alpha>1$, $n\sin\alpha>1$. We assume that magnetic permittivity $\mu=1$ as in [23] and hence $n^2=\epsilon$ (ϵ dielectric permittivity).

Field inside CR. We use Fresnel formulas for light wave reflection from plane boundary between dielectric and vacuum using complex reflection coefficient $R_\perp$ [23] (for the case of complete internal reflection):

$$R_\perp(\beta)=\frac{n\cos\beta-i\sqrt{n^2\sin^2\beta-1}}{n\cos\beta+i\sqrt{n^2\sin^2\beta-1}}$$

where β is incident angle. The sum field after two reflections from both facets *inside* dielectric is the following:

$$E_z=E_0\left(e^{-ik_x x-ik_y y}+R_\perp(\alpha)e^{+ik_x x-ik_y y}+\right. \tag{D1}$$
$$+R_\perp(\pi/2-\alpha)e^{-ik_x x+ik_y y}+$$
$$\left.+\;R_\perp(\pi/2-\alpha)R_\perp(\alpha)e^{+ik_x x+ik_y y}\right),$$
$$k=\frac{\omega}{c},\quad k_x=kn\cos\alpha,\quad k_y=kn\sin\alpha \tag{D2}$$

The first terms in brackets describe the incident wave, the second and third terms — the waves reflected from planes ($y=0$) and ($x=0$) correspondingly, the last term describes wave double reflected from both planes.

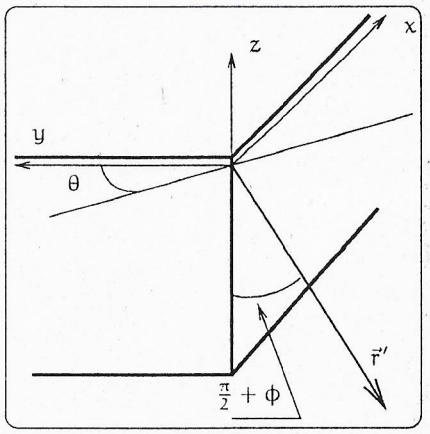

FIG. 7:

We simplify formula (D1) and calculate magnetic field:

$$E_z = 4E_0 e^{-i(\delta_x+\delta_y)} \cos(k_x x - \delta_x)\, \cos(k_y y - \delta_y), \tag{D3}$$

$$\tan\delta_x = \frac{\sqrt{n^2\sin^2\alpha - 1}}{n\cos\alpha}, \quad \tan\delta_y = \frac{\sqrt{n^2\cos^2\alpha - 1}}{n\sin\alpha} \tag{D4}$$

The field on outside surface of CR Now we can write down the expressions for fields outside CR in planes $x = 0-\epsilon$, $y = 0-\epsilon$ using boundary conditions — continuity of tangent component of $\vec{E}$ and normal component $\mu\vec{H}$. Then the expressions for fields are the following:

$$\begin{aligned}
E_z^{x=0} &= 4E_0 e^{-i(\delta_x+\delta_y)} \cos(\delta_x)\, \cos(k_y y - \delta_y),\\
H_x^{x=0} &= 4in E_0 \sin\alpha\, e^{-i(\delta_x+\delta_y)} \cos(\delta_x)\, \sin(k_y y - \delta_y),\\
H_y^{x=0} &= i4n E_0 \cos\alpha\, e^{-i(\delta_x+\delta_y)} \sin(\delta_x)\, \cos(k_y y - \delta_y),\\
E_z^{y=0} &= 4E_0 e^{-i(\delta_x+\delta_y)} \cos(k_x x - \delta_x)\, \cos(\delta_y),\\
H_x^{y=0} &= -4in E_0 \sin\alpha\, e^{-i(\delta_x-\delta_y)} \cos(k_x x - \delta_x)\, \sin(\delta_y),\\
H_y^{y=0} &= -4in E_0 \cos\alpha\, e^{-i(\delta_x+\delta_y)} \sin(k_x x - \delta_x)\, \cos(\delta_y)
\end{aligned}$$

We take in mind that plane wave is limited by Gaussian multiplier

$$b = \exp\Big(-a^2\big([x\sin\alpha - y\cos\alpha]^2 + z^2\big)\Big)$$

with small parameter a, or more precisely: $a \ll k$.

Radiation field. We can apply diffraction Green formula to E_z and calculate it in far wave zone in direction characterized by angles ϕ, θ and distance $|\vec{r}-\vec{r}'|$ (see fig.7):

$$E_z(\vec{r}') = \int \Big(E_z \partial_n G(R) - G(R)\partial_n E_z\Big)\, d\vec{r}, \tag{D5}$$

$$G(R) = \frac{e^{ikR}}{4\pi R}, \quad R = |\vec{r}' - \vec{r}| \gg \frac{1}{k}, \tag{D6}$$

$$\partial_n G(R) \simeq -ikG(R) \times \frac{\vec{n}(\vec{r}' - \vec{r})}{R}. \tag{D7}$$

Here $\vec{r}'$ is radius-vector of observation point, $\vec{r}$ is radius-vector of point on surface of integration, $d\vec{r}$ is element of integration surface, $\vec{n}$ is normal to surface of integration.

The result of calculations is the following:

$$E_z(R) = \frac{iE_0\, e^{ikr'}\, e^{-i(\delta_x+\delta_y)}}{\pi R} \times \tag{D8}$$

$$\times \underbrace{\frac{\sqrt{\pi}\, e^{-k^2\sin^2\phi/4a^2}}{a}}_{f(k\phi)\to\delta(k\phi)} \times \Big(I_x + I_y\Big),$$

$$I_x = kb_x \int_0^\infty dx\, \cos(k_x x - \delta_x) e^{ikx\cos\theta}\, e^{-a^2x^2\sin^2\alpha} \simeq$$

$$\simeq \frac{b_x\big(n\cos\alpha\,\sin\delta_x - i\cos\theta\,\cos\delta_x\big)}{n^2\cos^2\alpha - \cos^2\theta}, \tag{D9}$$

$$I_y = kb_y \int_0^\infty dy\, \cos(k_y y - \delta_y)\, e^{iky\sin\theta}\, e^{-a^2y^2\cos^2\alpha} \simeq$$

$$\simeq \frac{b_y\big(n\sin\alpha\,\sin\delta_y - i\sin\theta\,\cos\delta_y\big)}{n^2\sin^2\alpha - \sin^2\theta} \tag{D10}$$

Above we used auxiliary formulas:

$$I_c(k) = \int_0^\infty \cos kx\, e^{-a^2x^2}\, dx \;\Rightarrow\; \pi\delta(k), \quad \text{if } a \ll k, \tag{D11}$$

$$I_s(k) = \int_0^\infty \sin kx\, e^{-a^2x^2}\, dx \;\Rightarrow\; \frac{1}{k}, \quad \text{if } a \ll k,$$

Power of diffraction losses W can be calculated as following

$$W = \int_{-\pi/2}^{\pi/2}\int_{-\pi/2}^{\pi} \frac{|E_z|^2 c}{2\pi} R^2 \cos\phi\, d\phi\, d\theta = \frac{E_0^2 c}{2\pi^3} \times \frac{2\sqrt{\pi}}{ka} \times A,$$

$$A = \int_{-\pi/2}^{\pi} \big(I_x + I_y\big)^2\, d\theta \tag{D12}$$

We have to compare the value W with total power W_0 of incident wave

$$W_0 = \frac{E_0^2 c}{2a^2}, \qquad (1-R)_d = \frac{W}{W_0} = \frac{2a}{\pi^2\sqrt{\pi}k} \times A, \tag{D13}$$

Replacing notations $a \to 1/\sqrt{2}\,R_b$ and calculating numerically integral $A \simeq 32.8$ for $n = 1.45$ (SiO_2) and $\alpha = \pi/4$ we finally obtain the estimate (4.1).

APPENDIX E: TD TEMPERATURE FLUCTUATIONS IN THERMO-ISOLATED LAYER

We have thermal conductivity equation for temperature $u(\vec{r}, t)$ in infinite layer with width l ($0 \le z \le l$) with fluctuating force in right part [9] and the following boundary conditions:

$$\frac{\partial u}{\partial t} - a^2\Delta u = F(\vec{r}, t), \tag{E1}$$

$$\left.\frac{\partial u(\vec{r}, t)}{\partial z}\right|_{z=0,\,l} = 0, \tag{E2}$$

$$\langle F(\vec{r}, t)F(\vec{r}', t')\rangle = -\frac{2\kappa k_B T^2}{(\rho C)^2}\Delta\delta(\vec{r} - \vec{r}')\,\delta(t - t'), \tag{E3}$$

where $a^2 = \kappa/\rho C$, k_B is Boltzmann constant, δ is Dirac delta function.

We find solution as series:

$$u(\vec{r},t) = \iiint_{-\infty}^{\infty} \frac{dk_x\,dk_y\,d\omega}{(2\pi)^3} \sum_n u_n(k_x,k_y,\omega)\times$$
$$\times\, e^{i\omega t - ik_x x - ik_y y}\cos b_n z,$$
$$u_n(k_x,k_y,\omega) = \frac{F_n(k_x,k_y,\omega)}{i\omega + a^2(b_n^2+k_\perp^2)},$$
$$b_n = \frac{\pi n}{l}, \quad k_\perp^2 = k_x^2 + k_y^2,$$
$$u_n(k_x,k_y,\omega) = \iiint_{-\infty}^{\infty} dx\,dy\,dt\,e^{-i\omega t + ik_x x + ik_y y}\times$$
$$\times \int_0^l dz\,\frac{2-\delta_{0,n}}{l}\cos b_n z\, u(x,y,z,t),$$

We find correlation functions of coefficients $F_n(k_x,k_y,\omega)$:

$$F_{n,n_1} = \langle F_n(k_x,k_y,\omega)F^*_{n_1}(k_{x_1},k_{y_1},\omega_1)\rangle =$$
$$= \frac{2(2\pi)^3 k_B T^2 \kappa}{(\rho C)^2}\left(k_\perp^2 + b_n^2\right)\frac{2-\delta_{0,n}}{l}\,\delta_{n,n_1}\times$$
$$\times\,\delta(k_x - k_{x_1})\,\delta(k_y - k_{y_1})\,\delta(\omega-\omega_1).$$

We are interested in temperature $\bar{u}(t,x_0,y_0)$, averaged over volume $V = \pi R_b^2 l$ along axis parallel to axis z with transversal coordinates x_0 and y_0, and also its correlation function $\langle \bar{u}(t,0,0)\bar{u}(t+\tau),x_0,y_0\rangle$ with spectral density $S_{\bar{u}}(\omega)$:

$$\bar{u}(t,x_0,y_0) = \frac{1}{\pi R_b^2 l}\int_0^l dz \iint_{-\infty}^{\infty} dx\,dy\times$$
$$\times\, u(\vec{r},t)e^{-\frac{(x-x_0)^2+(y-y_0)^2}{R_b^2}} =$$
$$= \int_0^l \frac{dz}{l}\iint_0^\infty \frac{dx\,dy}{\pi R_b^2} e^{-\frac{(x-x_0)^2+(y-y_0)^2}{R_b^2}}\times$$
$$\times \iiint_{-\infty}^{\infty}\frac{dk_x\,dk_y\,d\omega}{(2\pi)^3}\sum_n u_n(k_x,k_y,\omega)\times$$
$$\times\cos b_n z\, e^{i\omega t - ik_x x - ik_y y} =$$
$$= \iiint_{-\infty}^{\infty}\frac{dk_x\,dk_y\,d\omega}{(2\pi)^3} e^{-\frac{R_b^2 k_\perp^2}{4}}\times$$
$$\times\, e^{i\omega t - ik_x x_0 - ik_y y_0}\,u_0(k_x,k_y,\omega), \qquad \text{(E4)}$$

$$B_{\bar{u}}(\tau) = \langle \bar{u}(t,0,0)\bar{u}(t+\tau,x_0,y_0)\rangle =$$
$$= \frac{2k_B T^2\kappa}{(\rho C)^2}\frac{1}{l}\iiint_{-\infty}^{\infty}\frac{dk_x\,dk_y\,d\omega}{(2\pi)^3}\times$$
$$\times\, e^{-\frac{R_b^2 k_\perp^2}{2} - ik_x x_0 - ik_y y_0}\frac{k_\perp^2 e^{i\omega\tau}}{\omega^2 + a^4 k_\perp^4} =$$
$$= \frac{k_B T^2}{(\rho C)}\frac{1}{\pi R_b^2 l(1+2a^2\tau/R_b^2)}\,e^{-\frac{x_0^2+y_0^2}{2(R_b^2+2a^2\tau)}}, \qquad \text{(E5)}$$

$$S_{\bar{u}}(\omega) = 2\int_{-\infty}^{\infty} d\tau\, e^{i\omega\tau}\langle \bar{u}(t,0,0)\bar{u}(t+\tau,0,0)\rangle =$$
$$= \frac{4k_B T^2\kappa}{(\rho C)^2 l}\int_0^\infty \frac{k_\perp\,dk_\perp}{2\pi}\,e^{-\frac{R_b^2 k_\perp^2}{2}}\frac{k_\perp^2}{\omega^2 + a^4 k_\perp^4} \qquad \text{(E6)}$$

Making following substitutions

$$\xi = \frac{k_\perp^2 R_b^2}{2}, \quad w = \frac{\omega R_b^2}{2a^2}, \quad a^2 = \frac{\kappa}{\rho C} \qquad \text{(E7)}$$

one can express the spectral density using exponential integrals:

$$S_{\bar{u}}(\omega) = \frac{k_B T^2}{\pi\rho C l\, a^2}\int_0^\infty \frac{\xi\,d\xi}{w^2+\xi^2}\,e^{-\xi} =$$
$$= \frac{k_B T^2}{2\pi\rho C l\, a^2}\times$$
$$\times\left(e^{iw}Ei_1(iw) + e^{-iw}Ei_1(-iw)\right),$$
$$Ei_n(x) = \int_1^\infty e^{-xt}\frac{dt}{t^n}$$

For particular cases this formula can be simplified:

$$S_{\bar{u}}(\omega)|_{w\ll 1} \simeq \frac{4k_B T^2\kappa}{(\rho C)^2 l}\,\frac{1}{\pi R_b^4\omega^2}, \qquad \text{(E8)}$$

$$S_{\bar{u}}(\omega)|_{w\gg 1} \simeq \frac{4k_B T^2}{\rho C\pi R_b^2 l}\times\frac{r_T^2}{R_b^2\omega}. \qquad \text{(E9)}$$

The formulas (E8 and E9) refer to non-adiabatic and adiabatic cases correspondingly.

APPENDIX F: PARAMETERS

For our estimates we used the following parameters, material parameters correspond to fused silica.

$$\omega = 2\pi\times 100\ s^{-1}, \quad \lambda = 1.064\ \mu m, \quad T = 300\ K,$$
$$b = 2.3\ cm, \quad R_b \simeq 6\ cm$$
$$m = 4\times 10^4\ g, \quad L = 4\times 10^5\ cm;$$
$$\alpha = 5.5\times 10^{-7}\ K^{-1}, \quad \kappa = 1.4\times 10^5\ \frac{erg}{cm\ s\ K},$$
$$\rho = 2.2\ \frac{g}{cm^3}, \quad C = 6.7\times 10^6\ \frac{erg}{g\ K},$$
$$n = 1.45, \quad \beta = \frac{dn}{dT} = 1.5\cdot 10^{-5}\ K^{-1}$$

[1] J. Ye, D. E. Vernooy and H. J. Kimble, "Trapping of single atoms in cavity QED", quant-ph/9908007.
[2] H. J. Kimble, private communication.
[3] G. Rempe et al, *Opt. Letters*, **17**, 363 (1992).
[4] A. Abramovici et al, *Science* **256**, 326 (1992).
[5] A. Abramovici et al, *Phys. Letters.* **A218**, 157 (1996).
[6] V. B. Braginsky and F. Ya. Khalili, *Quantum Measurement*, ed. by K.S. Thorne, Cambridge Univ. Press, 1992.
[7] V. B. Braginsky and F. Ya. Khalili, *Rev. Mod. Physics*, **68**, 1 (1996).

[8] F. Ya. Khalili, *Physics Letters* **A317**, 169 (2003)
[9] V. B. Braginsky, M. L. Gorodetsky, and S. P. Vyatchanin, *Physics Letters* **A 264**, 1 (1999); cond-mat/9912139;
[10] V. B. Braginsky and S. P. Vyatchanin, *Physics Letters* **A312**, 244 (2003);
arXiv: cond-mat/0302617,
[11] C. Cagnoli, D. Crooks, M. M. Fejer, Gregg Harry, Jim Hough, Norio Nakagawa, Steve Penn, Roger Route, Sheila Rowan, P. Sneddon, LIGO document: G030195-00, (2003)
[12] M. M. Fejer, S.Rowan, D. Crooks, P. Sheddon, G. Harry, J. Hough, S. Penn, to be published in *Phys.Rev.D.*
[13] V.B.Braginsky, A.A. Samoilenko, *Physics letters* **A315**, 175 (2003), arXiv:gr-qc/0304100v1.
[14] V. B. Braginsky, M. L. Gorodetsky, F. Ya. Khalili and K. S. Thorne, *Report at Third Amaldi Conference, Caltech*, July, 1999.
[15] Benvenuto Cellini, Autobiography, Penguin Books Ltd, 1956.
[16] Izwin I. Shapiro et al, Phys. Rev. Lett. **36**, 555 (1976);
J. G. Williams et al, Phys. Rev. Lett. **36**, 551 (1976).
[17] V. B. Braginsky, M. L. Gorodetsky, and S. P. Vyatchanin, *Physics Letters* **A 271**, 303-307 (2000)
[18] A. E. Siegman, Lasers, Univ. Science Book, 1996, ch. 19
[19] LIGO-II conceptual project book. LIGO document M990288-A1, available on www.ligo.caltech edu.
[20] E. d'Ambrosio, R. O'Shaughnessy, S. Strigin, K.Thorne and S. Vyatchanin, Reducing Thermoelastic Noise in Gravitational-Wave Interferometers by Flattening the Light Beams, submitted to *Phys. Rev. D*,
available as file beamreshape020903.pdf at http://www.cco.caltech.edu/~kip/ftp/
[21] O'Shaughnessy, S. Strigin and S. Vyatchanin, The implifications of Mexican-hat mirrors: calculations of thetmoelastic noise and interferometer sensitivity to perturbation for Mexican-hat mirror proposal for advanced LIGO, submitted to *Phys. Rev. D.*
[22] Garrilynn Billingsley, private communication.
[23] L. D. Landau and E. M. Lifshitz, Electrodinamics of continious media, Moscow, 1982. sec. 86.
[24] D.R.Crooks, P.Sneddon, G.Gagnoli, J.Hough, S.Rowan, M.M.Fejer, E.Gustavson, R.Route, N.Nakagawa, G.M.Harry, A.M.Gretarsson, to be published in *Classical and Quantum Gravity.*
[25] D.R.Crooks et al, *Classic and Quantum Gravity*, **19**, 4229, (2002).
[26] G. Harry et al, et al, *Classic and Quantum Gravity*, **19**, 897, (2002).
[27] S. Penn et al, *Classic and Quantum Gravity*, **20**, 2917, (2003).
[28] N. Nakagawa et al, Phys. Rev. D, **65**, 102001, (2002).
[29] Numata eat al *Phys.Rev.Lett.* **91**, 260602 (2202).
[30] E. Black et al, submitted to *Phys.Rev.Lett.*